Optical Engineering 49(2), 025001 (February 2010)

Design and analysis of a conceptual wavelength-division multiplexing optical network based on self-similarity

Shu-Tsung Kuo
Ming-Seng Kao
National Chiao-Tung University
Department of Communication Engineering
1001 Ta Hsueh Road
Hsinchu, 300 Taiwan
rogerkuo13@gmail.com

Abstract. We propose a novel multilevel wavelength-division multiplexing optical network based on the concept of self-similarity to simplify network structure and operation. Our approach lies on a simple network topology as well as an efficient wavelength management scheme being uniformly applied to all network levels. The proposed network is a compound packet-switched and wavelength-routed network with packet switching performed on the bottom level and wavelength routing on all upper levels. This network retains the efficiency of packet-switched networks and the simplicity of wavelength-routed networks. Switching operations are concentrated at some special nodes in the multilevel network, significantly simplifying the node configuration and wavelength routing. Moreover, the idea of λ bands is applied to unify wavelength management on all network levels. Network analysis is performed to assess the feasibility of our approach. A queueing model using the quality of service enhanced optical burst switching protocol is employed to analyze the blocking performance of the proposed network. Also, the numerical results based on the queueing model are provided. [DOI: 10.1117/1.3309456]

Subject terms: wavelength-division multiplexing optical network; dual-ring network; self-similarity; λ-band; optical burst switching; blocking probability.

Paper 090436R received Jun. 15, 2009; revised manuscript received Nov. 25, 2009; accepted for publication Dec. 10, 2009; published online Feb. 19, 2010.

1 Introduction

Continuous improvements to optical components and system technologies have allowed fibers to deliver several Tbits/sec data via wavelength-division multiplexing (WDM). The introduction of WDM has dramatically increased point-to-point transmission capacity and generated considerable potential to realize broadband all-optical networks.[1–5] The numerous wavelength carriers simultaneously transmitted along a fiber are valuable resources of photonic networks. Indeed, the ability to transmit hundreds of wavelengths along a single-mode fiber makes a high-capacity WDM network feasible.

In principle, the function of WDM optical networks is simple: to route specific wavelength carriers from source nodes to appropriate destinations. In practice, however, WDM optical networks are rather complicated. A large communication network is generally a hierarchical structure consisting of multiple network levels; the unique merits of different network levels should be considered in network design. This work proposes a multilevel WDM network architecture using the concept of self-similarity. Our idea stems from the fact that if a simple structure can be reproduced horizontally on the same level and vertically on different levels, it eventually becomes a complex structure that can accommodate related complexities, as is the case in the field of fractal geometry in mathematics[6] or cellular automata in computer science.[7] This idea of self-similarity enables us to integrate different network levels via the same approach to construct a simple and efficient multilevel WDM network. Note that this work intends to propose an idea that will likely be of interest in future wide-area WDM network designs, while the details involved in practical situations are not discussed.

To implement the proposed network architecture, basic issues associated with WDM optical networks must be considered. First, the principal function of WDM networks, as mentioned, is to route wavelengths along lightpaths offered by optical fibers. Thus, the network topology defined by fiber interconnections is a critical issue in network design. Second, an efficient wavelength management scheme is needed to route wavelengths adequately and efficiently in the network. Therefore, wavelength management (including wavelength assignment, wavelength routing, wavelength reuse, and wavelength conversion) is another issue that must be addressed.[8–10] Hence, this work is focused on designing a simple network topology and an efficient wavelength management scheme that can be applied to all network levels and can accommodate the varied requirements of different levels.

The remainder of this paper is organized as follows. Section 2 introduces the network hierarchy and operation principle. Next, for brevity sake, Sec. 3 presents a design example to illustrate the proposed wavelength management scheme. Section 4 demonstrates a bufferless approach for priority switching in source and destination switch fabrics, and their blocking performance is analyzed. Section 5 dis-

0091-3286/2010/$25.00

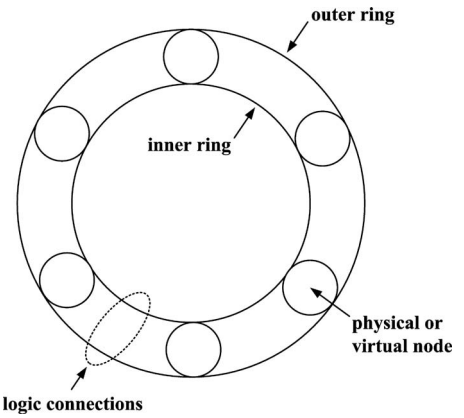

Fig. 1 Dual-ring network topology.

cusses some interesting features of the conceptual WDM network. Finally, conclusions are given in Sec. 6.

2 Network Hierarchy and Operation Principle

2.1 *The Cell*

On the physical layer, a WDM optical network is composed of many fibers with a number of wavelength carriers propagating along them. The interconnection of fibers, i.e., the network topology, defines the lightpaths through which wavelength carriers can propagate. Thus, the first step in our design was to find a network topology that could be applied to all network levels. Owing to the simplicity we desired, we did not consider some complicated topologies such as Shufflenet and Manhattan street network (MSN).[11,12] Instead, simple topologies like ring, star, bus, and tree topologies were considered. The star topology has been intensively studied,[13,14] but its inherent weakness in survivability makes it unsuitable for high-capacity networks. Also, it is difficult to practically implement a star network covering a wide area. Both the bus and tree topologies have been employed in local-area networks and subscriber loops, but they are also not suitable for wide-area networks. In contrast, the ring topology can cover a wide area, and the loop-back protection for it can be performed easily.[15–18] Therefore, we chose the ring topology.

To accommodate the varied requirements of different network levels, the special ring topology shown in Fig. 1 was designed with all the nodes within the dual-ring structure connected by an inner ring and an outer ring. We call such a dual-ring network a "cell." The idea of a cell was adopted from wireless communications, in which a cell uses a specific frequency band to deliver messages.[19] As will become clear in this paper, a dual-ring network in our approach uses specific wavelength bands (named λ bands) to deliver packets, and the dual-ring network is named a cell to distinguish it from common ring networks.

We considered a multilevel wide-area WDM network and applied the cell topology to all network levels. As shown in Fig. 1, a node in a cell can be a physical node or a virtual node. A physical node is a real node while a virtual node is actually a cell of the lower network level. On the bottom level, a cell consists of physical nodes only. On upper levels, a cell is generally composed of virtual nodes and/or physical nodes.

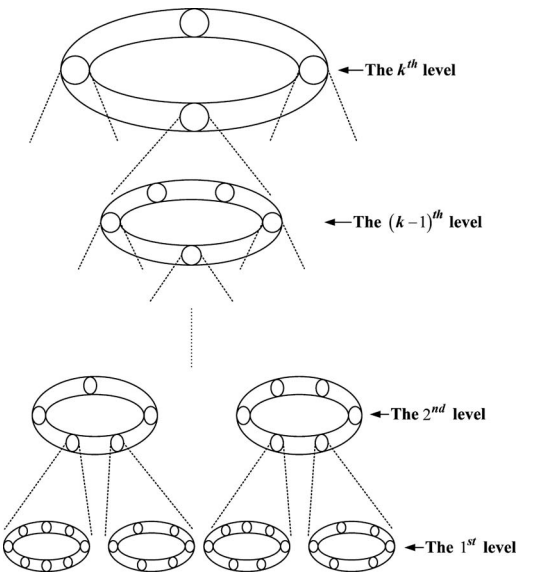

Fig. 2 Multilevel optical network consisting of *k* levels. The dual-ring topology is applied to all levels.

The neighboring nodes within the inner and outer rings of a cell have two connections between them that are named the "logic connections" (see Fig. 1). The logic connections can be specially implemented on different network levels. For example, depending on actual traffic and survivability requirements, two logic connections between neighboring nodes can be implemented by different fibers within a cable or by separate fiber cables. The introduction of virtual nodes and logic connections is aimed at providing a uniform topology while accommodating the varied requirements of different network levels. This idea will be clarified later.

Special nodes in each cell deliver wavelength carriers to and from the upper levels. We call these special nodes "edge nodes," and the others are "inner nodes." Edge nodes serve as bridges between adjacent network levels.

2.2 *Network Hierarchy*

We applied the idea of self-similarity to construct the multilevel optical network shown in Fig. 2. The network consists of *k* levels in which the first level is the bottom level and the *k*'th level is the top level. On the bottom level, a cell is composed of several physical nodes with logic connections between them. The logic connections provide lightpaths for packet transfer. There are many peer cells on this level (named "bottom cells") that form the basis of this wide-area network. A bottom cell is a basic unit in the network, and specific λ bands are assigned to each cell to deliver packets. A λ band is composed of a group of transmitting wavelengths of the corresponding cell. Each λ band is managed as a sole unit in the upper network levels, i.e., all wavelengths in a λ band are routed together and simultaneously. The detailed wavelength assignment and routing will be explained later.

The second level contains many level-2 cells that each consist of several nodes. A node on this level could be a virtual node or a physical node. A virtual node is actually a bottom cell. In reality, a physical node is a bigger node

whose traffic is comparable with a bottom cell. Although the constructions of physical nodes and virtual nodes are different, they are treated equally on this level. Again, specific λ bands were assigned to each level-2 cell as transmitting λ bands, where each is managed as a sole unit on the upper levels.

The same idea is applied to all the other levels. The resultant network is comprised of multiple levels in which each level consists of several cells and each cell has several nodes. Moreover, a virtual node on the j'th level is actually a cell of the $(j-1)$'th level. In practice, as the network level increases, the mean distance and the traffic between nodes increase.

The concept of virtual nodes and logic connections accomodates the varied requirements of different levels. For example, the coexistence of virtual nodes and physical nodes makes it easy to accommodate a single high-capacity node and the output of a group of low-capacity nodes together on the same level. To fulfill varied survivability and traffic demands, logic connections can be specially designed on different levels. Also, the number of nodes in every cell and the number of cells on different levels are specified by actual circumstances without special constraint.

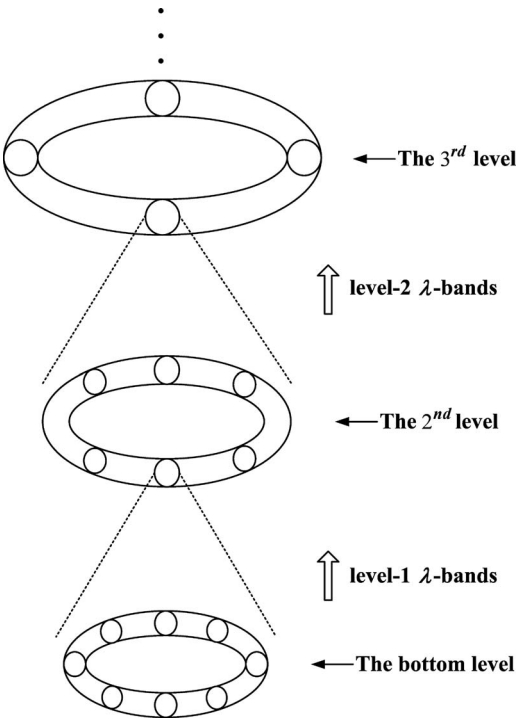

Fig. 3 Construction of λ bands on different levels. A level-j λ band is constructed on the j'th level and is delivered to the $(j+1)$'th level.

2.3 *Network Operation*

Before proceeding further, we will clarify whether the proposed network is a wavelength-routed network, a packet-switched network, or another network. A wavelength-routed network provides fixed lightpaths between source and destination pairs. The operation of wavelength-routed networks is simple, but a large number of wavelength carriers is required at each node, and the transmitter/receiver efficiency is poor. A packet-switched network is more efficient than a wavelength-routed network, but it requires high-speed photonic switches, optical delay lines for buffering, and overhead for routing processing, so its construction is more complicated.

Both packet-switched and wavelength-routed networks have their inherent advantages and drawbacks, so we adopted a compound scheme in our network by applying packet switching on the bottom level and simple wavelength routing on all upper levels. The use of packet switching significantly reduces the number of transmitters/receivers (TXs/RXs) needed at each node, while wavelength routing simplifies the operation of the upper levels.

Figure 3 depicts the operation of this optical network. On the bottom level, each node has several transmitters that send packets to all the other nodes in the whole network. The destination address is carried by the packet header. The optical packets generated by the nodes within a bottom cell are sent to edge nodes of this cell. At the edge nodes, those packets heading to destination nodes located at the same bottom cell are merged together by a switching system, then wavelength converted and grouped to be a λ band (named the level-1 λ band). Consequently, a bottom cell generates many level-1 λ bands, with each λ band carrying packets addressed to a specific bottom cell (including the mother cell itself). The level-1 λ band destined for the mother cell is delivered directly to the destination nodes, and the others are transferred to the second level. Each level-1 λ band is managed as a sole unit, which dramatically simplifies wavelength routing on the upper levels.

On the second level, a cell may consist of virtual nodes and physical nodes. A virtual node is actually a bottom cell whose outputs are level-1 λ bands. The outputs of a physical node are level-1 λ bands generated by itself. All the nodes within a cell deliver their outputs to edge nodes first, and then those level-1 λ bands destined for nodes in the same level-2 cell are merged as a level-2 λ band. Except for the particular level-2 λ band heading to the mother cell, the others are delivered to the third level and are individually managed as a sole unit on the upper levels.

The same operation as that of the second level is performed repeatedly on the third and other upper levels, which is the core idea of self-similarity. In general, a cell on the j'th level generates q_j level-j λ bands, where q_j is the total number of cells on this level. Each level-j λ band carries packets destined for a particular level-j cell. Except the level-j λ band addressed to the mother cell, the others are sent to the $(j+1)$'th level.

The typical trip that a packet would experience in such a network is shown in Fig. 4. A packet Z is generated by a source node (n_s) inside a bottom cell (C_s) and delivered to a destination node (n_d) located at another bottom cell (C_d). Packet Z starts the trip on the bottom level, being sent from the node n_s to an edge node of C_s. At the edge node, all packets heading to destination nodes inside C_d are switched together, wavelength converted, and then grouped to be a level-1 λ band. Afterward, the level-1 λ band containing packet Z is sent to the second level.

On the second level, the bottom cell C_s is treated as a virtual node belonging to a particular level-2 cell. The

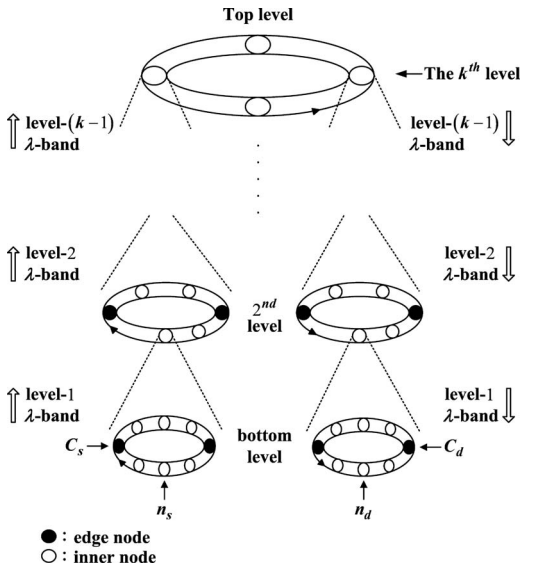

Fig. 4 Typical trip a packet will experience in the multilevel network from a source node n_s located at a bottom cell C_s to a destination node n_d located at the other bottom cell C_d.

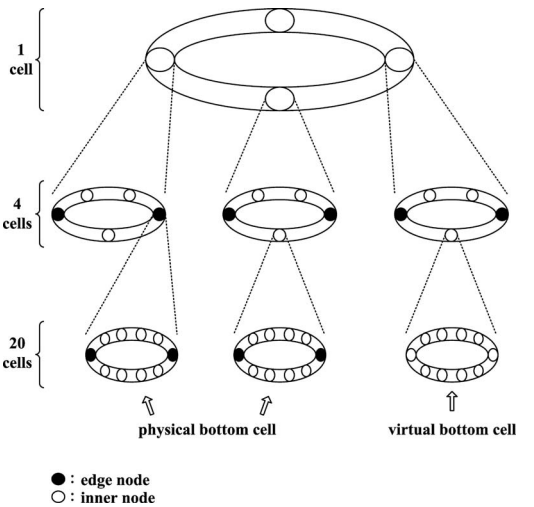

Fig. 5 Example of the three-level network.

level-1 λ band of interest is delivered to an edge node of this level-2 cell and merged with other level-1 λ bands destined for the level-2 cell containing C_d as a level-2 λ band. Next, this level-2 λ band is transferred to the third level, and the operation is repeated. Eventually packet Z arrives at the top level (the k'th level) and is contained by a specific level-$(k-1)$ λ band.

On the top level, the level-$(k-1)$ λ band with packet Z is sent directly from the (virtual) node containing C_s to the node containing C_d. Afterward, the level-$(k-1)$ λ band is transferred to the $(k-1)$'th level, then decomposed into several level-$(k-2)$ λ bands. The level-$(k-2)$ λ band with packet Z would be dropped by a node that includes C_d. Afterward, this level-$(k-2)$ λ band is delivered to the $(k-2)$'th level and decomposed into several level-$(k-3)$ λ bands. The same process is repeated all the way to the bottom level.

On the bottom level, the level-1 λ band containing packet Z is accepted by an edge node of C_d. At the edge node, packet Z is switched and wavelength converted to be the receiving wavelength of n_d. Finally, packet Z is carried by the corresponding receiving wavelength and eventually accepted by n_d.

In the above description of our network, a packet is switched twice in the network. The switching operation in the source cell makes a node able to use few transmitters to send packets to all the nodes in the network. It achieves the same transmitter efficiency as a packet-switched network. The switching operation in the destination cell enables a node to use few receivers to accept packets coming from all the nodes in the network, and it also has the same receiver efficiency as a packet-switched network. These two switching operations take full advantage of the benefits of packet switching, but unlike common packet-switched networks, the packet-switching operations are concentrated at some edge nodes in our network and are absent elsewhere.

An implicit advantage of our design is that a blocking problem can occur only on the bottom level, which ensures an excellent quality of service (QoS). The blocking problem for the proposed network will be studied in detail in Sec. 4.

3 Wavelength Management Scheme

In this section, the wavelength management scheme for our proposed network is investigated. For WDM optical networks, wavelengths are precious resources, so an efficient wavelength management scheme is necessary and it is critical to best use those available wavelengths. A limit on the number of wavelengths co-propagating along a single-mode fiber must be taken into account because it sets a practical constraint on wavelength management. The other issues that should be considered are wavelength reuse and wavelength conversion. The aim of an efficient wavelength management scheme is to maximize wavelength reuse while minimizing wavelength conversion.

For illustrative purposes, the example shown in Fig. 5 considers a WDM network consisting of three levels. For simplicity, we assume that the cells on the same level have an equal number of nodes. On the top level, there is only one cell with four virtual nodes inside. On the second level, there are four cells that each consist of five virtual/physical nodes. On the bottom level, there are 20 cells that each have 10 nodes. As shown in the figure, a physical node on the second level is treated as a virtual cell on the bottom level. In the following discussion, this example is used to illustrate the network construction and wavelength management.

3.1 *Bottom Level*

As shown in Fig. 6, the physical nodes in a bottom cell are connected with a fiber cable. Since the effect of fiber failure on the bottom level is less critical, one fiber cable is used to implement logic connections in the bottom cell. There are eight inner nodes and two edge nodes in the cell, and the traffic of this cell is managed by two edge nodes.

For the purpose of illustration we assume the traffic between any two bottom nodes is identical. Although this

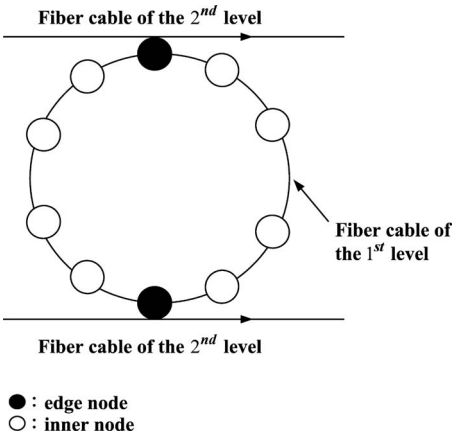

Fig. 6 Construction of a physical bottom cell in the example. The edge nodes are further connected to fiber cables of the second level.

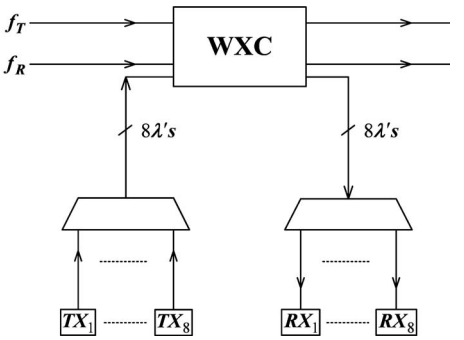

Fig. 7 Configuration of inner node.

simplified assumption is made here, the derived results can be easily applied to practical networks with suitable modifications.

Let $a_{\ell,i}$ be the number of nodes in the cell C_i on the ℓ'th level. The number of cells on the ℓ'th level, denoted as N_ℓ, is given by

$$N_l = a_{l+1,1} + a_{l+1,2} + \cdots + a_{l+1,N_{l+1}} = \sum_{i=1}^{N_{l+1}} a_{l+1,i}. \tag{1}$$

Let F_λ be the capacity of a wavelength carrier, and T_n be the node-to-node traffic on the bottom level. Due to the varied sizes of bottom cells on this level, the traffic between cell C_i and cell C_j on the bottom level, denoted as $T_{i,j}$, is calculated by

$$T_{i,j} = T_n \cdot a_{1,i} \cdot a_{1,j}, \quad i \neq j. \tag{2}$$

The intra-traffic of a bottom cell C_i can be obtained from Eq. (2) using the following modification:

$$T_{i,i} = T_n \cdot (a_{1,i} - 1) \cdot a_{1,i}. \tag{3}$$

Here we assume the traffic between C_i and C_j on the bottom level is an integer multiplier of the capacity of a wavelength carrier, i.e.,

$$T_{i,j} \approx Z_{i,j} \cdot F_\lambda, \tag{4}$$

where $Z_{i,j}$ is an integer. The total number of wavelengths required in a bottom cell C_i can be calculated as

$$W_{1,i} = Z_{i,1} + Z_{i,2} + \cdots \cdots + Z_{i,i} + \cdots \cdots + Z_{i,N_1} = \sum_{j=1}^{N_1} Z_{i,j}. \tag{5}$$

A bottom cell C_i needs $(W_{1,i} - Z_{i,i})$ wavelength carriers to communicate with the other bottom cells and $Z_{i,i}$ wavelength carriers for intra-cell traffic, respectively. Because of the varied scales of bottom cells, the total number of wavelengths needed in each cell is different.

If the required wavelength carriers are generated equally by all the nodes within a bottom cell C_i, the number of transmitters needed at each node is given by

$$m_{1,i} = \lceil W_{1,i}/a_{1,i} \rceil, \tag{6}$$

where "$\lceil x \rceil$" denotes the minimum integer equal to or greater than a real number x.

We can assign $m_{1,i}$ different wavelengths to each node in a physical bottom cell C_i. The $m_{1,i}$ wavelengths appointed to a particular node will be served as transmitting wavelengths as well as receiving ones because they are the identity wavelengths of this node. Consequently, the total number of wavelength carriers assigned to a bottom cell C_i is evaluated as

$$X_{1,i} = a_{1,i} \cdot m_{1,i}. \tag{7}$$

As will be clear soon, the same set of $X_{1,i}$ wavelength carriers can be reused in the other bottom cells without wavelength conflict, which unifies the optical components used in all the bottom cells.

To become familiar with the operation of a bottom cell, we must first consider the particular inner node n_i in a bottom cell C_i shown in Fig. 6. Let the output traffic of n_i be 80 Gbps and assume each TX can carry 10 Gbps information. Hence, eight transmitters (i.e., $m_{1,i}=8$) with different output wavelengths are equipped to deliver the traffic of n_i. These transmitters are divided into two groups, with each consisting of four transmitters. Since there are 20 bottom cells (including C_i itself) in the network example, each transmitter group of n_i will carry packets destined for 10 bottom cells. The outputs of two transmitter groups are separately sent to two edge nodes.

The configuration of n_i is shown in Fig. 7. All transmitting wavelengths are added to the transmitting fiber (f_T), and all receiving wavelengths are dropped from the receiving fiber (f_R) via the wavelength cross-connect (WXC). The structure and operation of the inner node are quite simple, which can be easily implemented in practice.

The configuration of the edge node is shown in Fig. 8. As described above, an edge node will receive four wavelengths coming from each of the other nine nodes of this cell (eight inner nodes and one edge node) plus four wavelengths locally generated by itself. Thus, a total of 40 wavelengths destined for 10 bottom cells will be managed by it. Without loss of generality, these 40 wavelengths are de-

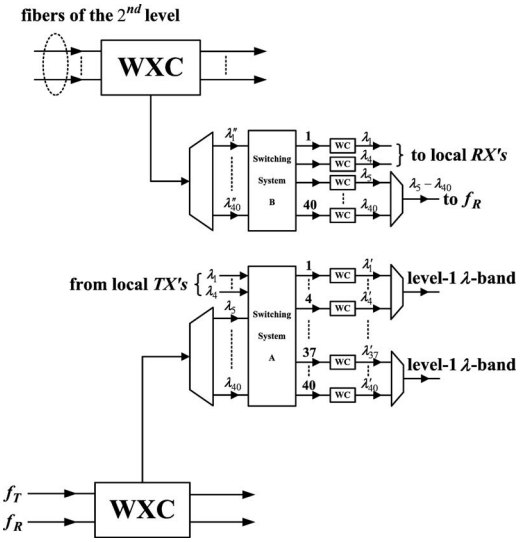

Fig. 8 Configuration of edge node.

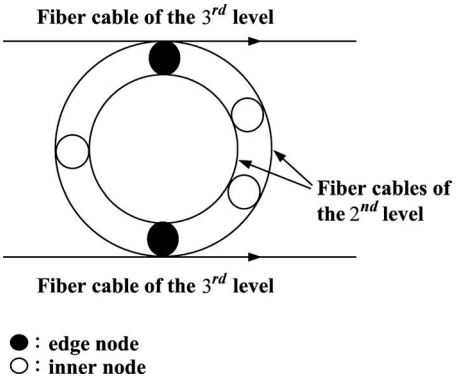

Fig. 9 Construction of a level-2 cell in the example. The edge nodes are further connected to fiber cables of the third level.

noted as $(\lambda_1-\lambda_{40})$, in which wavelengths $(\lambda_1-\lambda_4)$ are locally generated and wavelengths $(\lambda_5-\lambda_{40})$ are delivered from the other nine nodes of this cell.

As shown in Fig. 8, wavelengths $(\lambda_5-\lambda_{40})$ are dropped from the transmitting fiber via a WXC and then decomposed into individual wavelengths by a WDM demultiplexer. The 36 incoming wavelengths plus four local wavelengths are sent to a photonic switching system A. The switching system has 40 ingress and 40 egress ports. Recall that the packets destined for the 10 bottom cells are carried by these 40 wavelengths, so the 40 output ports are divided into 10 groups. Each group consists of four egress ports that correspond to a particular destination bottom cell. According to the addresses carried by the packet headers, those packets destined for the same bottom cell are switched together to the corresponding egress group. A wavelength converter (WC) is placed at each egress port to convert the output packets to a particular wavelength. The four wavelengths of each output group are further merged to be a level-1 λ band. Thereafter, 10 level-1 λ bands are constructed with each consisting of four different wavelengths, so a total of 40 wavelengths $(\lambda_1'-\lambda_{40}')$ is generated. Each level-1 λ band carries packets heading to a specific bottom cell.

The edge node shown in Fig. 8 also accepts 10 level-1 λ bands coming from the second level that carry packets destined for this bottom cell, so a total of 40 wavelengths $(\lambda_1''-\lambda_{40}'')$ is received. These received level-1 λ bands are first decomposed into individual wavelengths and then sent to a photonic switching system B. This switching system also has 40 ingress and 40 egress ports. Since the receiving wavelengths carry packets destined for 10 nodes in this cell, the 40 egress ports are divided into 10 groups. Each group consists of four ports, that correspond to a particular node in the bottom cell. Those packets heading to a particular node will be switched to the four egress ports assigned to this node. A WC is placed at each egress port to convert the output into a specific wavelength.

Although the structure of an edge node is more complicated, just two edge nodes are needed in a bottom cell. Moreover, switching and wavelength conversion are performed only at edge nodes and therefore are absent at inner nodes on the bottom level.

Each level-1 λ band is composed of wavelengths destined for a particular bottom cell. Moreover, a specific level-1 λ band destined for the intracell traffic within the mother bottom cell is generated in a physical bottom cell but will not be created in a virtual bottom cell. Assume that $b_{1,i,j}$ is the number of wavelengths in a level-1 λ band dedicated to cell C_i to cell C_j traffic. According to the preceding description, we can obtain $b_{1,i,j}$ by

$$b_{1,i,j} = Z_{i,j} = \left\lceil \frac{T_n \cdot a_{1,i} \cdot a_{1,j}}{F_\lambda} \right\rceil. \tag{8}$$

All the level-1 λ bands generated in a bottom cell will be delivered to the second level except the one carrying packets destined for those nodes within the mother cell. This specific level-1 λ band heading to the mother cell will be sent directly to destination nodes. Therefore, for a bottom cell, a total of (N_1-1) level-1 λ bands are transferred to the second level.

3.2 *Second Level*

A typical level-2 cell is shown in Fig. 9. The inner ring and outer ring of this cell are implemented by two separate fiber cables. There are two edge nodes in the cell that deal with wavelengths carried by the inner ring and outer ring fiber cables, respectively. As was the case on the bottom level, the number of edge nodes in a level-2 cell also depends on the amount of traffic within this cell.

From the preceding discussion, a node on this level will output (N_1-1) level-1 λ bands. The function of this level is to merge those level-1 λ bands destined for the same level-2 cell as a level-2 λ band and deliver them either to the upper levels or directly to destination nodes in the mother cell. Since the node-to-node traffic on this level is equivalent to a level-1 λ band, the number of wavelength carriers contained in a level-2 λ band can be calculated.

Let $a_{2,p}$ be the number of nodes in cell C_p on the second level. In general, the number of wavelengths in a level-2 λ band can be formulated as

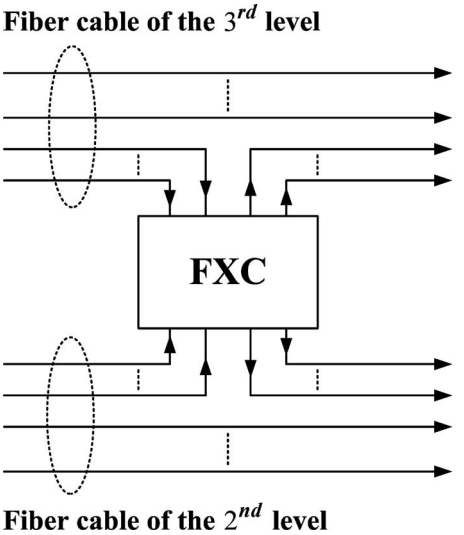

Fig. 10 Configuration of an edge node on the second level.

$$b_{2,x,y} = \sum_{i=1}^{a_{2,x}} \sum_{j=1}^{a_{2,y}} b_{1,i,j}, \tag{9}$$

where $b_{1,i,j}$ is the number of wavelengths in the level-1 λ band used for the traffic from node n_i in cell C_x to node n_j in cell C_y on the second level. For the particular level-2 λ band addressed to nodes in the mother cell, the number of wavelengths within it is evaluated as

$$b_{2,x,x} = \sum_{i=1}^{a_{2,x}} \sum_{\substack{j=1 \\ j \neq i}}^{a_{2,x}} b_{1,i,j}. \tag{10}$$

From Eqs. (9) and (10), we obtain the total number of transmitting wavelengths to be delivered by cell C_x as

$$W_{2,x} = \sum_{y=1}^{N_2} b_{2,x,y}. \tag{11}$$

The level-2 cell shown in Fig. 9 illustrates the operation inside the cell. The cell of interest is named $C_{2,x}$ and its outer ring is considered first. There are $a_{2,x}$ nodes within $C_{2,x}$ and each node outputs r (=10 in this example) level-1 λ bands to the outer ring, so a total of $(a_{2,x} \cdot r)$ level-1 λ bands will be carried. These level-1 λ bands will be sent to an edge node and be managed by it. At the edge node, those level-1 λ bands destined for the same level-2 cell are merged as a level-2 λ band. With deliberate wavelength assignment, those level-1 λ bands heading to K (=2 here) particular level-2 cells can be carried by the outer fiber cable of $C_{2,x}$. The number of wavelength carriers contained in each of the level-2 λ bands separately delivered to the K level-2 cells can be obtained by Eq. (9).

The wavelengths belonging to K level-2 λ bands are separately carried by K fibers, and those level-1 λ bands heading to the same level-2 cell are naturally merged as a level-2 λ band in the transmitting fiber cable. The construction of the edge node is shown in Fig. 10. Here, a fiber cross-connect (FXC) instead of a WXC is used, thereby transmitting the K level-2 λ bands generated by this cell to the upper level, and K level-2 λ bands coming from other cells are dropped from the upper level.

3.3 *Upper Levels*

In each cell of the second level, there are N_2 level-2 λ bands being generated, in which (N_2-1) of them are sent to the other level-2 cells and one of them is destined for the mother cell. On the third level, a level-2 cell is regarded as a virtual node. The outputs of each node on this level are (N_2-1) level-2 λ bands, and each level-2 λ band is managed as a sole unit. An operation similar to that of the second level is performed.

From the above discussion, we see that as the network level increases, the number of wavelengths contained in a λ band increases, whereas the number of λ bands to be processed decreases. A λ band is managed as a sole unit, which implies that the higher the network level, the fewer the number of λ bands that are managed and the simpler the routing operation becomes.

4 Performance Analysis

In the proposed multilevel WDM network, a transmitting packet may be dropped in the switching systems during its delivery. This section describes the just-enough-time (JET) based optical burst switching (OBS) model we used to analyze the blocking performance of the switching systems on a packet path from a source cell to a destination cell.[20–22] In principle, the OBS system works as follows. Arriving data packets are assembled into much larger bursts in advance and then fed into the switching entity. Under the reservation mechanism of JET, each burst is preceded by a corresponding control packet in the time domain, and their respective transmission instants at the source node are separated by a time interval called an offset. The control packet is electronically processed at the switching system in its source and destination cells but the burst is not, so the offset time between them compensates for the processing delay of the control packet. A control packet contains information about the length of its corresponding burst, the value of the offset time between them, and the routing scheme. When it arrives at a switching system in the source/destination cell, it would request resource allocation in the switch for its corresponding burst. If the requested bandwidth resource is available, it is reserved from the time the burst is expected to arrive until the time the burst leaves the switch, which makes the burst transparently pass through the switch fabric. Otherwise, the burst would be blocked and dropped.

To provide service differentiation in OBS, one feasible approach is to assign different offset values for different burst traffic classes. As described in Refs. 20–22, a longer offset allows higher-priority traffic to reserve resources prior to lower-priority traffic with a shorter offset, which gives the better QoS to higher-priority burst traffic. Such a mechanism of service differentiation for separate traffic classes was applied to our OBS model. For the sake of brevity, our analyses are conducted in accordance with the network example demonstrated in Sec. 3, whose focus is on the blocking performance of the switching systems A and B shown in Fig. 8. Since an OBS burst is an aggregation of

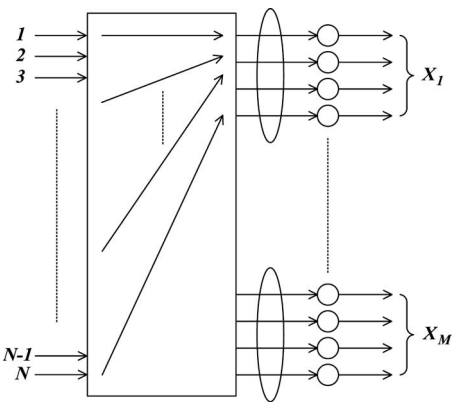

Fig. 11 QoS-enhanced OBS model for the switching system A/B.

many data packets, the packet loss probability of our OBS model can be inferred from its burst loss probability.

A JET-based, service-differentiation-supporting OBS model for the switching system A/B is investigated and depicted in Fig. 11. No buffering is provided. In this model, we consider two service priority classes, i.e., class 1 and class 2, where the bursts of class 1 have preemptive priority over those of class 2. The N output ports of this switch are divided into M groups according to the number of bottom cells/nodes being managed. Those output ports in each group are further multiplexed to an output link. The parameter X_z denotes the number of output ports in the group z, where $z=1,2,\cdots,M$, which is the number of wavelengths in a λ band carried by their attached output link. We assume that the class-mixed burst arrivals for a concerned output link follow a Poisson process.

In the following analyses, we first focus on a specific (i.e., tagged) output link of the switching system A, which serves an output group z. We assume that the class m arrival rate for the tagged output link is α_m and its service rate is β_m, where $m=1,2$. Because the bursts of class 1 have strict priority over those of class 2, the blocking probability of class 1 bursts for the tagged output link can be calculated by using the well-known Erlang B formula, as addressed in Refs. 20 and 21, given by

$$P_1^A = \frac{\rho_1^{X_z}/X_z!}{\sum_{k=0}^{X_z} \rho_1^k/k!}, \tag{12}$$

where $\rho_1(=\alpha_1/\beta_1)$ is the traffic load of class 1.

The mixed traffic of classes 1 and 2 is possessed of absolute service priority in this two-class OBS system; therefore, the blocking probability of the mixed traffic for the tagged output link can be obtained, independent of service differentiation, as

$$P_{\text{mixed}}^A = \frac{\rho^{X_z}/X_z!}{\sum_{k=0}^{X_z} \rho^k/k!}, \tag{13}$$

where $\rho=\rho_1+\rho_2=(\alpha_1/\beta_1)+(\alpha_2/\beta_2)$. Note that we have assumed the mean burst lengths of class 1 and class 2 are equal for the equality in Eq. (13).

Using P_1^A and P_{mixed}^A, we can acquire the burst blocking probability of class 2, P_2^A, by solving the following equality:

$$(\alpha_1+\alpha_2)\cdot P_{\text{mixed}}^A = \alpha_1 \cdot P_1^A + \alpha_2 \cdot P_2^A. \tag{14}$$

It is formulated as follows:

$$P_2^A = \frac{\alpha_1+\alpha_2}{\alpha_2} P_{\text{mixed}}^A - \frac{\alpha_1}{\alpha_2} P_1^A, \tag{15}$$

where α_1 and α_2 represent the class 1 and class 2 arrival rates for the tagged output link of switching system A, respectively.

The process to estimate the blocking performance for switching system B is similar to that for switching system A; however, the effective arrival rates of class 1 and class 2 at the switching system B, α_1' and α_2', are reduced to $\alpha_1'=(1-P_1^A)\alpha_1$ and $\alpha_2'=(1-P_2^A)\alpha_2$, respectively, due to the blocking impact at the switching system A. Let β_m' be the class m service rate of switching system B and assume $\beta_m'=\beta_m$, where $m=1,2$. Since $\alpha_m'=(1-P_m^A)\alpha_m$, we have $\rho_m'=(\alpha_m'/\beta_m')=(1-P_m^A)\rho_m$.

Using the effective traffic loads and above assumption, the blocking probabilities of class 1 and mixed traffic, on a considered output link of the switching system B, can be calculated as

$$P_1^B = \frac{(\rho_1')^{X_z}/X_z!}{\sum_{k=0}^{X_z} (\rho_1')^k/k!} = \frac{[(1-P_1^A)\rho_1]^{X_z}/X_z!}{\sum_{k=0}^{X_z} [(1-P_1^A)\rho_1]^k/k!} \tag{16}$$

and

$$P_{\text{mixed}}^B = \frac{(\rho')^{X_z}/X_z!}{\sum_{k=0}^{X_z} (\rho')^k/k!}, \tag{17}$$

where $\rho'=\rho_1'+\rho_2'=(1-P_1^A)\rho_1+(1-P_2^A)\rho_2$. Then the blocking probability of class 2 bursts is

$$\begin{aligned} P_2^B &= \frac{\alpha_1'+\alpha_2'}{\alpha_2'} P_{\text{mixed}}^B - \frac{\alpha_1'}{\alpha_2'} P_1^B \\ &= \frac{(1-P_1^A)\alpha_1+(1-P_2^A)\alpha_2}{(1-P_2^A)\alpha_2} P_{\text{mixed}}^B - \frac{(1-P_1^A)\alpha_1}{(1-P_2^A)\alpha_2} P_1^B. \end{aligned} \tag{18}$$

While delivering a class m burst toward the destination cell in this network example, its overall blocking probability is obtained as

$$P_{BL,m} = 1-(1-P_m^A)(1-P_m^B) = P_m^A + P_m^B - P_m^A \cdot P_m^B, \quad m = 1,2. \tag{19}$$

Two simulation results based on the network example for the overall blocking probabilities of class 1 and class 2 versus the normalized utilization with different values of $\gamma(\triangleq \rho_2/\rho_1)$ are plotted in Figs. 12 and 13, respectively. In the simulation, the parameter X_z is set to be 4, and $\beta_1=\beta_2=\beta_1'=\beta_2'$. In these two figures, note that for a given γ,

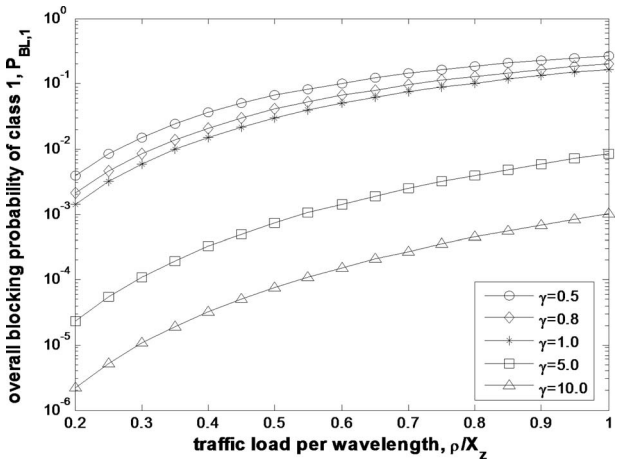

Fig. 12 Overall blocking probability of class 1 versus the traffic load per wavelength with different values of γ. The parameter $X_z=4$.

the lower-priority traffic (i.e., class 2 burst traffic herein) has the higher blocking probability, as expected. Because the service priority of class 1 is always higher than that of class 2, and for a given ρ the traffic load of class 1 decreases as γ increases, the blocking probability of class 1 bursts reduces significantly when γ is large. Thus, the variation of γ would result in greater influence on $P_{BL,1}$ than on $P_{BL,2}$. To operate the network at a high utilization with low blocking probabilities of class 1 and class 2, the ratio of ρ_2 to ρ_1, i.e., γ, should be large; however, it implies that limited high-priority traffic is allowed in the network. Therefore, a tradeoff exists between the amount of high-priority traffic and the blocking performance when designing such a multilevel WDM network.

5 Discussion

The concept underlying self-similarity is a simple geometric structure enabled by a recursive algorithm. By repeatedly expanding (or shrinking) the geometric structure using the recursive algorithm, a complicated object can be obtained. This object has the unique feature that a part of it is exactly or approximately similar in shape to itself.

This paper describes how we applied the idea of self-similarity to design a multilevel WDM network. This conceptual WDM network has some interesting features:

- It is self-similar in network topology. A level-j cell has several nodes inside it. If we look into one of the nodes, a cell structure similar to the level-j cell appears. However, the level-j cell becomes a (virtual) node on the $(j+1)$'th level, and the level-$(j+1)$ cell has a cell structure similar to that of the level-j cell. Thus, this property unifies network topology on different levels.
- It is self-similar in λ bands. A level-j λ band consists of several level-$(j-1)$ λ bands. If we look into a level-$(j-1)$ λ-band, it is similarly composed of several level-$(j-2)$ λ bands. Several level- j λ bands can be merged to become a level-$(j+1)$ λ band. Owing to the self-similarity property of λ bands, wavelength routing is simplified, which requires us to simply merge or decompose λ bands on each level without addressing individual wavelengths.
- It is a compound packet-switched and wavelength-routed network. In the proposed optical network, packet switching is performed on the bottom level, which can much enhance the TX/RX efficiency. The switching of transmitting wavelengths involves merging the transmitted packets together to construct level-1 λ bands. The switching of receiving wavelengths involves merging the incoming packets addressed to the same destination node together. Without these switching operations, a large number of transmitters/receivers will be required in each node. Meanwhile, simple wavelength routing is carried out on all upper levels, which significantly simplifies network operations.

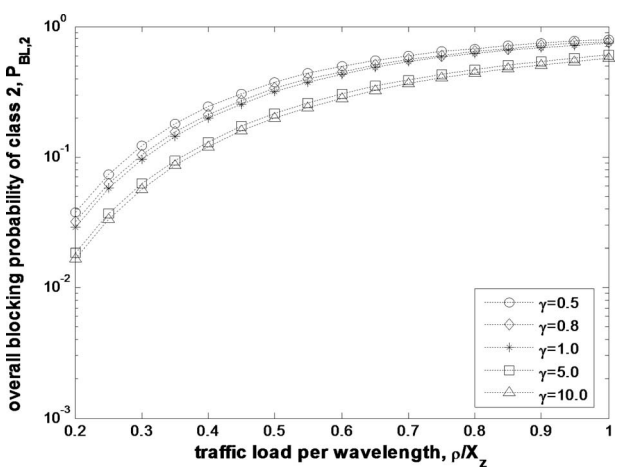

Fig. 13 Overall blocking probability of class 2 versus the traffic load per wavelength with different values of γ. The parameter $X_z=4$.

6 Conclusions

In this paper, we have proposed a novel network architecture based on self-similarity for multilevel wide-area WDM networks. We developed special dual-ring topology and an efficient wavelength management scheme that can be applied to all network levels. The dual-ring structure offers great flexibility and assures good survivability in the event of fiber failure. The idea of λ bands is introduced to efficiently manage wavelength carriers. In the proposed optical network, packet switching is performed at edge nodes of the bottom level, while simple wavelength routing on λ bands is carried out on upper levels. Therefore, the proposed architecture retains the efficiency of packet-switched networks and the simplicity of wavelength-routed networks. The performance analysis of the proposed multilevel WDM optical network showed that, according to our numerical results, the parameters for designing such a WDM network can be appropriately determined.

References

1. P. Green, "Progress in optical networking," *IEEE Wireless Commun. Mag.* **39**, 54–61 (2001).
2. B. Mukherjee, "WDM optical communication networks: progress and

challenges," *IEEE J. Sel. Areas Commun.* **18**, 1810–1824 (2000).
3. A. H. Gnauck, R. W. Tkach, A. R. Chraplyvy, and T. Li, "High-capacity optical transmission systems," *J. Lightwave Technol.* **26**, 1032–1045 (2008).
4. T. Ohara, H. Takara, T. Yamamoto, H. Masuda, T. Morioka, M. Abe, and H. Takahashi, "Over-1000-channel ultradense WDM transmission with supercontinuum multicarrier source," *J. Lightwave Technol.* **24**, 2311–2317 (2006).
5. H. Suzuki, M. Fujiwara, and K. Iwatsuki, "Application of super-DWDM technologies to terrestrial terabit transmission systems," *J. Lightwave Technol.* **24**, 1998–2005 (2006).
6. H. M. Kastings and G. Sugihara, *Fractals: A User's Guide for the Nature Science*, Oxford University Press, Oxford, UK (1993).
7. T. Toffoli and N. Margolus, *Celluar Automata Machines*, MIT Press, Cambridge, Massachusetts (1987).
8. P. Saengudomlert, E. Modiano, and R. G. Gallager, "On-line routing and wavelength assignment for dynamic traffic in WDM ring and torus networks," *IEEE/ACM Trans. Netw.* **14**, 330–340 (2006).
9. B. Wen, R. Shenai, and K. Sivalingam, "Routing, wavelength and time-slot-assignment algorithms for wavelength-routed optical WDM/TDM networks," *J. Lightwave Technol.* **23**, 2598–2609 (2005).
10. A. Mokhtar and M. Azizoglu, "Adaptive wavelength routing in all-optical networks," *IEEE/ACM Trans. Netw.* **6**, 197–206 (1998).
11. M. Gerla, E. Leonardi, F. Neri, and P. Palnati, "Routing in the bidirectional shufflenet," *IEEE/ACM Trans. Netw.* **9**, 91–103 (2001).
12. W. T. Lee and L. Y. Kung, "Binary addressing and routing schemes in the Manhattan street network," *IEEE/ACM Trans. Netw.* **3**, 26–30 (1995).
13. X. Lu, J. Chen, and S. He, "Wavelength assignment method for WDM network of star topology," *Electron. Lett.* **40**, 625–626 (2004).
14. O. Moriwaki, K. Noguchi, and Y. Sakai, "Physically asymmetric star network with CWDM wavelength router," *IEEE Commun. Lett.* **11**, 188–190 (2007).
15. W. T. Anderson et al., "The MONET project—A final report," *J. Lightwave Technol.* **18**, 1988–2009 (2000).
16. J. Manchester, P. Bonenfant, and C. Newton, "The evolution of transport network survivability," *IEEE Wireless Commun. Mag.* **37**, 44–51 (1999).
17. G. Sacchi, S. Sugliani, A. Bogoni, F. D. Pasquale, R. D. Muro, R. Magri, G. Bruno, and F. Cavaliere, "Design and experimental characterization of EDFA-based WDM ring networks with free ASE light recirculation and link control for network survivability," *J. Lightwave Technol.* **23**, 1170–1181 (2005).
18. S. B. Park, C. H. Lee, S. G. Kang, and S. B. Lee, "Bidirectional WDM self-healing ring network for hub/remote nodes," *IEEE Photon. Technol. Lett.* **15**, 1657–1659 (2003).
19. T. S. Rappaport, *Wireless Communications, Principles and Practice*, Prentice Hall, Upper Saddle River, New Jersey (1996).
20. H. L. Vu and M. Zukerman, "Blocking probability for priority classes in optical burst switching networks," *IEEE Commun. Lett.* **6**, 214–216 (2002).
21. K. Dolzer and C. Gauger, "On burst assembly in optical burst switching networks—A performance evaluation of just-enough-time," in *Proc. Int. Teletraffic Congr. (ITC17)*, Vol. **4**, pp. 149–160 (2001).
22. M. Yoo, C. Qiao, and S. Dixit, "QoS performance of optical burst switching in IP-over-WDM networks," *IEEE J. Sel. Areas Commun.* **18**, 2062–2071 (2000).

Shu-Tsung Kuo received BS and MS degrees in electrical engineering from Yuan-Ze University, Taiwan, R.O.C., in 1996 and 1999, respectively. He is currently working toward his PhD degree in the Department of Communication Engineering, National Chiao-Tung University, Hsinchu, Taiwan. His main research interest is in high-speed optical networks.

Ming-Seng Kao received his BSEE degree from National Taiwan University in 1982, his MS degree in optoelectronics from National Chiao-Tung University in 1986, and his PhD degree in electrical engineering from National Taiwan University in 1990. From 1986 to 1987 he was an assistant researcher at the Telecommunications Laboratories, Chung-Li, Taiwan. In 1990, he joined the faculty of National Chiao-Tung University, Hsinchu, Taiwan, where he is now a professor in the Communication Engineering Department. From 1993 to 1994, he was a visiting professor at the Swiss Federal Institute of Technology (ETH), Zurich, Switzerland, where he worked in the area of optical communications. He is currently interested in high-speed optical networks and wireless communications.